Fast response MPPT charger for the Técnico Solar Boat

Afonso Daniel Guerreiro Coelho

Introduction to the Research in

Electrical and Computer Engineering

Supervisors: Gonçalo Nuno Gomes Tavares
Pedro Rafael Bonifacio Vitor

January 2026

Abstract

Solar-powered vehicles rely on solar energy to charge their batteries and maximize their range, particularly solar-powered boats need an effective energy conversion in rapidly changing environmental conditions. In this context, the Maximum Power Point Tracker (MPPT) charger plays a critical role in energy conversion, by ensuring that the solar panels operate on their Maximum Power Point (MPP) while charging a battery. This work focus on the study, design, simulation and test of a fast response MPPT charger for Técnico Solar Boat (TSB).

This document contains the State-of-the-Art review covering photovoltaic principles, MPPT algorithms, DC-DC converter topologies, charging techniques, processing units, and commercial solutions. Special attention is given to the algorithms suitable for dynamic conditions, and DC-DC topologies.

Based on the conduct study and the project requirements, a solution was proposed capable of effectively convert energy, operating the solar panels on their MPP, and without compromising the product cost. Preliminary simulations were conduct to validate the software tools chosen and gain familiarity with the given tools. The ultimate objective of this project is to develop a reliable, efficient, and customizable MPPT solution that improves energy extraction, enhances system monitoring through CAN communication, and contributes to the overall performance and competitiveness of the TSB.

Keywords: MPPT, MPPT topology, DC-DC Converter, Solar energy, P&O, Solar Boat

Contents

Acronyms

ASIC   Application-Specific Integrated Circuit

BMS   Battery Management System

CAN   Controller Area Network

CC   Constant Current

CV   Constant Voltage

DC   Direct Current

FPGA   Field Programmable Gate Array

GUI   Graphical User Interface

IC   Integrated Circuit

IncCond   Incremental Conductance

MCU   Microcontroller Unit

MPP   Maximum Power Point

MPPT   Maximum Power Point Tracker

LUT   Look-Up Table

OTS   Off the shelf

P&O   Perturb and Observe

PCB   Printed Circuit Board

PV   Photovoltaic

R&D   Research and Development

SG01   São Guabriel 01

STC   Standard Testing Conditions

TSB   Técnico Solar Boat

1 Introduction

1.1 Motivation

With environmental pollution intensifying worldwide, the transition to cleaner energy sources such as solar power has become increasingly urgent. In 1985, only 20.82% of the energy produced in the world came from renewable energies. These numbers have been rising every year, and in 2024, have reached 31.92% [1]. In 2024, 6.9% of the energy produced in the world comes from solar panels, and in Portugal this number rises to 14.5%, demonstrating the importance and the impact of solar energy [1]. Solar energy still plays a minuscule role, and it is listed behind the other sources of energy in terms of its contribution to meeting the world's energy demand. However, solar energy is becoming more relevant, with the cost of solar panels dropping significantly in the last decade.

In comparison to other forms of green energy, Photovoltaic energy is relevant due to its availability, simplicity, lower maintenance, environmental friendliness, reliability, and many other benefits. More recently, it is becoming more relevant in the automotive industry, with solar-powered cars, boats, and robots [2]. The CO2 emissions of the automotive sector are one of the main contributors to global warming. In 2018, 29% of total CO2 emissions in the EU came from the transport sector, with 4% coming from the maritime sector alone [3]. These challenges have directly motivated the development of the Técnico Solar Boat (TSB) project.

In 2015, TSB was created with the goal of designing and building a solar-powered boat to compete in international competitions. Since then, the project has grown, and several vessels have been built. It began with the construction of the first solar prototype, São Rafael 01, which still had a lot of room for improvement and was followed by São Rafael 02 and 03. The team then decided to approach the hydrogen energy and autonomous driving, and therefore São Miguel 01 and 02 and São Pedro 01 were built. More recently, a vessel was built to combine all the technologies used before and was named São Guabriel 01 (SG01).

All these prototypes used solar energy to maximize their range and efficiency. In the first years the energy produced was small, and the whole system was built using commercial Off the shelf (OTS) components. In 2020, the team started to build its own solar panels for São Rafael 03. Many other systems were also designed and built in house, but there is still one system that is yet to be developed, the Maximum Power Point Tracker (MPPT) charger.

The MPPT charger is a fundamental subsystem in photovoltaic energy systems, responsible for maximizing the power extracted from solar panels by ensuring continuous operation at the Maximum Power Point (MPP). A MPPT charger is typically a power converter that continuously monitors the voltage and current produced by the photovoltaic modules and adjusts their electrical operating point accordingly. By dynamically regulating these operating parameters, the MPPT compensates for variations in environmental conditions such as solar irradiance and temperature, which cause the MPP to shift over time. As a result, the photovoltaic system can operate with improved efficiency and deliver maximum available power under changing conditions [4].

1.2 Objectives

This project aims to design and implement a MPPT charger for the solar panels used in TSB project. The MPPT charger will convert the energy produced by the solar panel as efficiently as possible with the use of a quality DC-DC converter and the implementation of MPP tracking algorithms.

The main objectives of this project are:

- Study and understand the operation of solar panels and MPPT techniques;

- Choose the most suitable DC-DC topology for the system;

- Implement a fast response and accurate control algorithm;

- Design and simulate the hardware and software;

- Implement the system in hardware and develop a Printed Circuit Board (PCB);

- Test and validate the performance of the circuit;

- Ensure the safety and reliability of the MPPT charger for its integration in the TSB project;

- Provide performance data of the solar panel and the MPPT through a Controller Area Network (CAN) communication interface.

By achieving these objectives, the project will contribute to a more efficient solar system, maximizing the energy received from the solar panels and increasing the available data for performance tracking of the MPPT and solar panel. This data will be used to later improve the energy efficiency of the MPPT and take conclusions about the manufacture quality of the solar panels build by TSB project. A cheap, efficient and versatile MPPT will also mean future savings to the team, since it could be used in a variety of vessels.

1.3 Outline

This document is organized into five main chapters:

- **Chapter 1** introduces the context of the work, presenting the motivation behind the development of an MPPT charger for the TSB project. The objectives of the project are defined, and the scope of the proposed solution is established;

- **Chapter 2** presents the State-of-the-Art related to photovoltaic energy systems and MPPT technology. It reviews the operating principles of solar panels, solar energy production, and the most relevant MPPT algorithms. Additionally, different DC-DC converter topologies, battery charging techniques, processing units, and commercial solutions are analyzed and compared;

- **Chapter 3** describes the proposed solution for the MPPT system. The overall system architecture is presented, followed by a summary of the technical requirements. The adopted design approach and methodology are detailed, including converter selection, control strategy, simulation, and experimental validation plan;

- **Chapter 4** presents the preliminary work developed so far, including initial simulations and early design results that support the feasibility of the proposed solution;

- **Chapter 5** outlines the planning and scheduling of the project, presenting the development timeline and key milestones required to achieve the defined objectives.

2

State-of-the-Art

In this chapter, the main State-of-the-Art concepts regarding the engineering behind an MPPT charger and solar panels are explained. More specifically, it addresses key challenges such as: what is a solar panel, MPPT algorithms, DC-DC converter types, and battery charging techniques.

2.1   Solar Panels

Photovoltaic (PV) panels are devices that convert solar irradiance into electrical energy. A PV panel consists of multiple solar cells electrically connected in series and/or parallel to achieve the desired voltage and current levels. As in conventional electrical systems, the interconnection topology directly affects the electrical characteristics of the panel: series connections increase the output voltage, while parallel connections increase the output current [5].

Series-connected PV panels operate at higher voltage levels, which reduces conduction losses in interconnecting cables and improves the efficiency of the DC-DC conversion stage. Moreover, power converters designed for high voltage and low current operation are generally less complex and more cost-effective than those operating at low voltage and high current. However, series configurations are more sensitive to partial shading or panel failure, as the output current of the entire string is limited by the weakest module [6]. In contrast, parallel configurations provide improved tolerance to shading and faults but result in higher current levels and increased conduction losses. In this project, series/parallel configuration of the solar panels will not be changed, since it is already pre-defined by Técnico Solar Boat (TSB), but it is important to understand the implications of each configuration.

Each cell is made of semiconductor materials, usually silicon. This semiconductor is doped with phosphorus, a group V element, to create a negative type layer. On the other side, a layer is doped with boron, a group III element, to create a positive type layer. This creates a p-n junction, which is essential for the photovoltaic effect [7].

When sunlight arrives at the solar cell, the photons energy is absorbed by the semiconductor material. This energy excites electrons, allowing them to escape their atomic bonds and create electron hole pairs. The electric field at the p-n junction drives these free electrons towards the n-type layer and holes towards the p-type layer, generating a flow of electric current when the cell is connected to an external circuit [7], Figure 2.1.
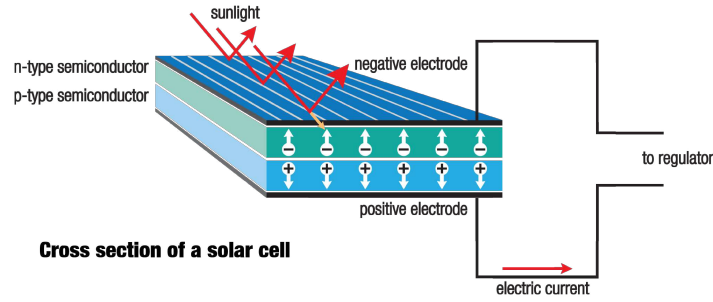
Figure 2.1: Principle of operation of a solar panel [8].

The energy generated results in voltage and current outputs that are not constant. Voltage and current are interdependent, therefore, a variation in one parameter leads to a corresponding variation in the other. This relationship is nonlinear and can be characterized by a current-voltage (I-V) curve. Furthermore, the power output also varies with operating conditions and can be represented by a power-voltage (P-V) curve. Both curves are represented in Figure 2.2. In both curves, there is a specific point where the power output is maximized, known as the Maximum Power Point (MPP). This point corresponds to a unique combination of voltage and current, denoted as V_{mpp} and I_{mpp}, respectively. Operating the solar panel at this point ensures optimal energy extraction under a given condition.
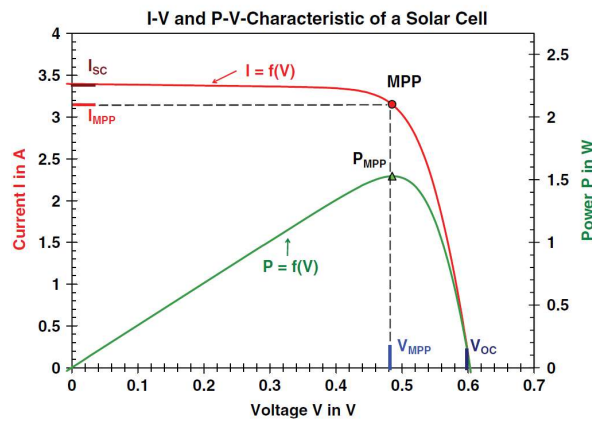

Figure 2.2: I-V and P-V curves of a solar panel [7].

The characteristic curves of a solar panel depend on various factors, including the quality of the materials used, the solar cells, and environmental conditions such as temperature, solar irradiance, wind, and shades. It is noted that under partial shading conditions, it is possible to have multiple local maxima, but overall, there is still only one true MPP [9].

As seen in Figure 2.3a, the variation of the solar irradiance changes the I-V and P-V curves of the solar panel. The increase in irradiance produces more power by mainly increasing the current output of the panel. On the other hand, the temperature has an opposite effect (Figure 2.3b). The increase in temperature produces a decrease in power output, mainly by decreasing the voltage output of the panel.

5
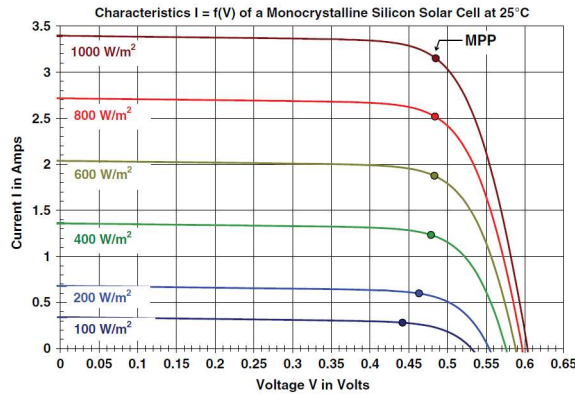
(a) Cell temperature of 25 ºC and variable Irradiance.
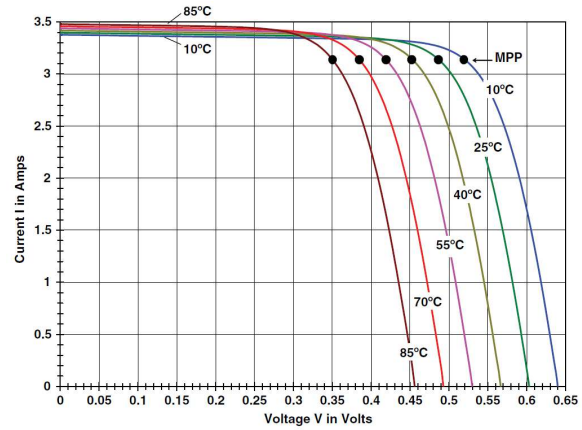
(b) Irradiance of $1\ \mathrm{kW/m^2}$ and variable temperature.

Figure 2.3: I-V curves under different conditions [7].

Both environmental conditions have a meaningful impact on the MPP of the solar panel and therefore on the power output of the system. To maximize the power extracted by the solar panels, a classic power converter, like a buck converter with fixed duty cycle, will not be efficient since neither the current nor the voltage are constant for different conditions. Instead, an MPPT charger is used, which will find the MPP and operate the solar panel at that point while sensing the changes caused by the environment.

2.2   Maximum Power Point Tracker (MPPT)

A Maximum Power Point Tracker (MPPT) charger is a device that is used to optimize the power output from solar panels by continuously tracking and adjusting the operation point of the panels to ensure they operate at their MPP.

To achieve its goal, an MPPT charger is usually composed of a DC-DC converter, a microcontroller, and some sensors (Figure 2.4). The sensors are used to measure the input/output variables of the control system (typically voltage and current). The information acquired by these sensors is processed by the microcontroller, which runs an algorithm to determine if the MPP was reached or how to act on the system towards the MPP. In the second case, the microcontroller generates a signal to control the DC-DC converter that will adjust its operation accordingly.

The output can be connected to different types of loads, like batteries, DC loads or inverters. This project focuses on batter charging applications.
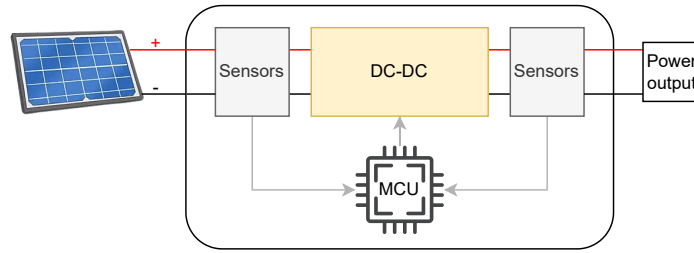
Figure 2.4: Simplified structure of an MPPT charger.

2.3 MPPT Algorithms

There are plenty of MPPT algorithms, each one with its own advantages and disadvantages. The choice of the algorithm will depend on the specific application, the desired performance, and the available resources. In this work, the aim is to extract the maximum energy possible of a solar panel installed in a moving boat, which will produce an I-V curve variation due to the quick changes in irradiance caused by changes of inclination, orientation and clouds, and also temperature changes due to waves and wind. For these reasons, tracking speed and accuracy are the most important factors to consider.

With this in mind, the most relevant algorithms are briefly reviewed in order to identify the most suitable option for this project.

2.3.1 Constant Voltage (CV)

This is the simplest and most inefficient method. It works by operating the solar panel at a fixed voltage. This referenced voltage is used to calculate the duty cycle of the DC-DC converter that will maintain the operating point of the solar panel.

Well-known variants improve performance by setting the reference voltage to a fraction of the open-circuit voltage (typically 71-78%) [9]. This voltage is obtained by briefly disconnecting the panel from the load, increasing reference accuracy and efficiency. Another variant uses a fraction of the short-circuit current as the reference [10].

Although both methods are simple and cost-effective, they are inherently inefficient due to the necessity of interrupting energy production during measurement phases. However, alternative implementations address this limitation through proxy measurement techniques employing dummy cells or diodes, whose physical properties closely approximate those of standard solar cells, thereby enabling continuous power generation during measurement acquisition [9] [11]. Still, the MPP is not always located at the same percentage of the open-circuit voltage or short circuit current, leading to a lack of accuracy and therefore lower efficiency [4].

7

2.3.2 Perturb and Observe (P&O)

The Perturb and Observe (P&O) method is widely used in commercial products and is the basis of many advanced algorithms. Its popularity lies in its simplicity, low cost, and ease of implementation.

As its name indicates, the algorithm perturbs the voltage of a PV array and observes the resulting effect on the output power [12]. If an increase in voltage leads to an increase in output power, the operating point is moving toward the MPP, and the algorithm continues to increase the voltage. Conversely, if the output power decreases, the operating point is moving away from the MPP, and the direction of the perturbation is reversed [13, 14]. Figure 2.5 illustrates the flowchart of the algorithm.

The biggest drawback of this algorithm is that it oscillates around the MPP, which produces power losses. This oscillation can be reduced by decreasing the step size of the perturbation, but this will also reduce the tracking speed of the algorithm. This results in an inherent trade-off between tracking speed and accuracy [9, 10].

To mitigate this issue, an adaptive step size can be used, where the step size is larger when the MPP is far away and smaller when it is closer. Consequently, the tracking speed is maximized while minimizing the oscillations around the MPP. This can be achieved by measuring the power and voltage and calculating the P-V curve slope ($\Delta P/\Delta V$). At the MPP, this slope approaches zero, allowing the step size to be reduced accordingly. This adaptive variant is commonly referred to as the differential power perturb-and-observe(dP-P&O)".

Another weal-know issue of P&O is that it can get confused in rapidly changing environmental conditions, like fast irradiance changes caused by clouds. In this case, the algorithm can misinterpret the power change caused by the environmental variation as a result of its own perturbation, leading it to move away from the MPP instead of towards it [9]. For example, if the perturbation was in the wrong direction, but the irradiance increased, the power output would increase, and the algorithm would continue perturbing in the wrong direction (Figure 2.6).
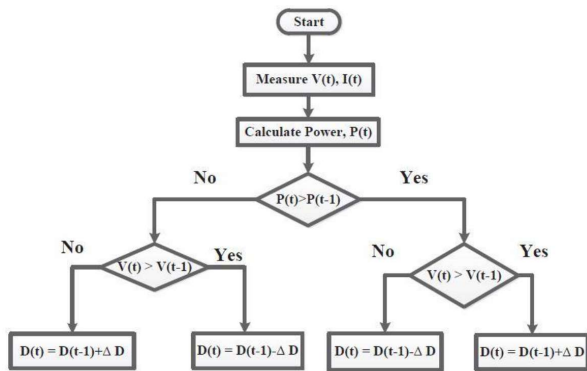

Figure 2.5: Flow chart of the classic version of Perturb and Observe algorithm [14].
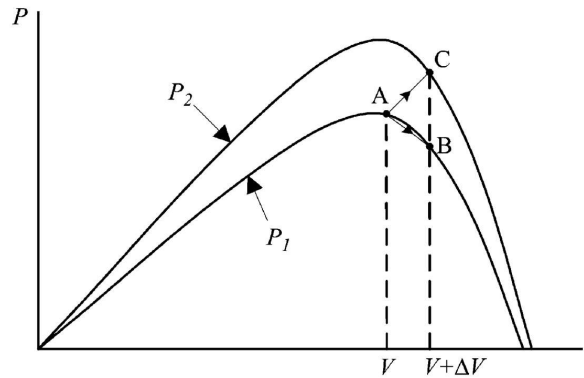
Figure 2.6: Divergence of P&O from MPP as shown in [15]

To address this limitation, an additional condition is incorporated into the algorithm that evaluates two consecutive measurements of ΔP and ΔV. Specifically, when the signs of consecutive ΔP measurements do not follow the signs of ΔV, this indicates that the observed power variation results from environmental disturbances rather than the algorithm's perturbation. Consequently, the voltage adjustment is suppressed. This refined variant is designated the two-point algorithm or improved P&O method [5].

There are other variations of P&O algorithm that improve its performance, like Variable Step Size P&O (VSS-P&O), the three-point P&O, a-factor P&O, and more. Unfortunately, due to the scope of this work, it is not possible to explain all of them.

2.3.3 Incremental Conductance (IncCond)

The Incremental Conductance (IncCond) algorithm is another widely used MPPT method due to its accuracy and ability to track the MPP under rapidly changing environmental conditions.

This algorithm is based on the fact that at the MPP, the derivative of power with respect to voltage is zero. By knowing the output voltage and current of the solar panel, the algorithm can calculate the conductance and the incremental conductance [16].

The following formulas, Equation 2.1, show the equation on which this algorithm is based.

$$\frac{dP}{dV} = \frac{d(V \cdot I)}{dV} = I + V\frac{dI}{dV} \rightarrow \frac{1}{V} \times \frac{dP}{dV} = \frac{I}{V} + \frac{dI}{dV} \tag{2.1}$$

At the MPP point, the slope of the P-V curve is zero, which means that the negative of the conductance, $-I/V$, is equal to the incremental conductance, dI/dV, (Figure 2.8). The algorithm compares these two values to determine if the operating point is at, to the left, or to the right of the MPP [10] [9]:

$$\frac{dP}{dV} = 0 \quad \Longleftrightarrow \quad \frac{dI}{dV} = -\frac{I}{V} \qquad \text{at MPP}$$

$$\frac{dP}{dV} > 0 \quad \Longleftrightarrow \quad \frac{dI}{dV} > -\frac{I}{V} \qquad \text{left of MPP} \tag{2.2}$$

$$\frac{dP}{dV} < 0 \quad \Longleftrightarrow \quad \frac{dI}{dV} < -\frac{I}{V} \qquad \text{right of MPP}$$

Based on these conditions, the algorithm adjust its operating point (increasing or decreasing the voltage) using a variable step size based on the instantaneous conductance relative to the incremental conductance, Figure 2.7. For example, as suggested in [9], the step size can be calculated using a proportional integral (PI) controller with zero as input reference and error defined as:

$$e = \frac{I}{V} + \frac{dI}{dV} \tag{2.3}$$

Comparative analysis demonstrates that the IncCond algorithm exhibits superior performance relative to the P&O method. This outcome is expected, as the Incremental Conductance technique was

developed specifically to address the limitations inherent in the P&O approach [16]. For example, the IncCond method eliminates the oscillation problem around the MPP that is characteristic of the P&O method. Additionally, IncCond demonstrates superior performance under rapidly changing environmental conditions, such as sudden irradiance variations, since it uses derivative-based information that is less sensitive to transient disturbances [5].
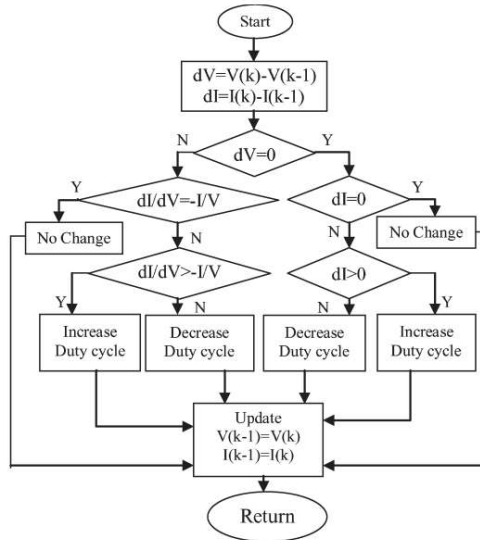
Figure 2.7: Flowchart of the IncCond method with direct control [17].
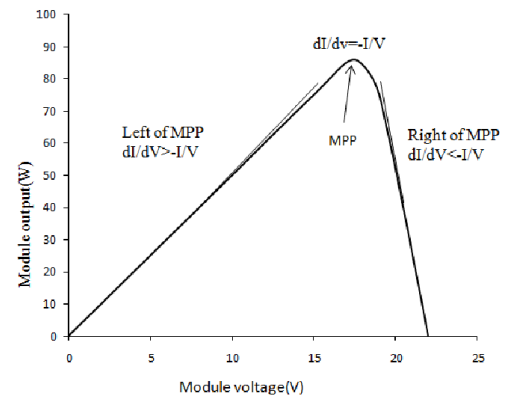
Figure 2.8: IncCond method principle.

2.3.4 Look Up Table (LUT)

The Look-Up Table (LUT) method is a simple and fast MPPT algorithm that relies on pre-calculated/measured data to determine the optimal operating point of a solar panel [10].

The LUT table contains several entries organized by voltage and current. Each of these entries contains the optimal duty cycle of the DC-DC converter, that are pre-calculated or measured for a specific voltage and current. This approach allows the algorithm to reach the MPP in one clock cycle by measuring the voltage and current of the solar panel, looking for the closest entry in the LUT table, and applying the corresponding duty cycle to the converter. The entries of the table can be calculated through a mathematical model of the solar panel with different conditions (temperature and irradiance) or measured in a laboratory.

Table 2.1 is a visual representation of a 2D LUT, only based on current and voltage. Each entry represents the duty cycle used in each case.

The main advantage of this method is its speed since it can reach the MPP in one clock cycle. This makes it suitable for applications where fast tracking is required, like in this project. However, it is not very accurate [14].

Table 2.1: LUT matrix representation with $m \times n$ elements.

	V_1	$\cdots$	V_k	$\cdots$	V_m
I_1	D_{11}	$\cdots$	D_{1k}	$\cdots$	D_{1m}
$\vdots$	$\vdots$		$\vdots$		$\vdots$
I_j	D_{j1}	$\cdots$	D_{jk}	$\cdots$	D_{jm}
$\vdots$	$\vdots$		$\vdots$		$\vdots$
I_n	D_{n1}	$\cdots$	D_{nk}	$\cdots$	D_{nm}

To improve the accuracy, the LUT table needs to be larger, which increases the required memory resources. Also, by adding the temperature and/or irradiance to the table would increase the accuracy, making it almost 100% accurate, but this would increase the size of the table exponentially. In extreme cases, the memory requirements became expensive and slow. There is a trade-off between size, speed, and accuracy that needs to be considered when using this method. Also, the LUT method does not adapt to the aging of the solar panel or changes in its characteristics over time, unless the table is updated periodically through new measurements.

2.4 Types of DC-DC Converters

The DC-DC converter is a crucial component of an MPPT charger, as it allows the adjustment of the operating point of the solar panel to match the MPP. His choice is highly important to the project since it directly affects the efficiency, cost, and complexity of the overall system.

DC-DC converters can be classified into two main categories: isolated and non-isolated converters. The main difference between these two types of converters is the presence or absence of galvanic isolation between the input and output circuits [18].

2.4.1 Non-isolated versus isolated DC-DC converters

This galvanic isolation is usually achieved by using a transformer, which provides electrical separation between the input and output sides of the converter. This isolation is important in applications where safety is a concern, such as in medical devices or industrial equipment, as it helps to prevent electrical shock and damage to sensitive components. In the context of solar energy systems and E-mobility, isolated converters are often used when the solar panel is connected to the grid [19], as they help to protect against voltage spikes and other electrical disturbances. Also, this converter can provide very higher/lower gain, which is useful for applications where solar panels MPP voltage is very different from the battery or load voltage (typically medium/high voltages).

In contrast, non-isolated converters do not provide galvanic isolation between the input and output

circuits. However, they generally offer higher efficiency, lower cost, reduced size, and lower circuit complexity (Table 2.2). Additionally, they present fewer challenges in thermal management and are simpler to design. These advantages, together with the fact that galvanic isolation is not a requirement for this application, led to the exclusion of isolated DC-DC converters from this project.

Table 2.2: Comparison between Non-isolated and isolated converters (undesired , medium and good characteristics are highlighted).

Type	Non-isolated Converters	Galvanic Isolated Converters
Circuit Complexity	Low	High
Efficiency	High	Medium
Size	Compact	Large
Electromagnetic Interference (EMI)	Medium/High	High
Switching Frequency	Medium	Medium
Thermal Management	Easier	Moderate
Control Complexity	Moderate	Moderate
Gain	Near 1	Very High/low
Cost	Low	High

2.4.2 Non-isolated DC-DC converters

Modern non-isolated conversion circuits generally use one of three basic topologies: buck, boost, or buck-boost converters. They are "basic" in the sense that only one switching element is needed. A given topology is used to obtain a specific result, such as voltage step-down, voltage step-up, or hybrid mode [20].

The **boost converter** is a step-up DC-DC converter widely employed in MPPT controllers when the required output voltage is higher than the solar panel open circuit voltage. It uses an inductor to store energy when the transistor is in the ON state and the diode is reverse-biased. When the transistor is on the OFF state, the inductor releases the stored energy to the output through the diode, increasing the output voltage (Figure 2.9b) [21].

This topology has been extensively documented in the literature and is distinguished by its inherent simplicity, cost-effectiveness, and superior efficiency characteristics [2] [14] [16]. Depending on the design variation used and constraints, it can achieve conversion efficiencies up to 98% [22].

A limitation of this topology is that it cannot emulate an impedance lower than the load impedance, which prevents it from reaching values close to the short-circuit current of the PV module. Consequently, it is not compatible with all solar panels or MPPT algorithms [22, 23].

The **buck converter** is a step-down DC-DC converter also widely used for applications where the solar panel voltage is higher than the battery or load voltage. Similar to the boost converter, it uses an inductor to store energy when the transistor is in the ON state and the diode is reverse-biased. However, in this case, the input is connected to the output when the transistor is in the ON state. When the transistor is in the OFF state, the inductor releases the stored energy to the output through the diode, decreasing the output voltage (Figure 2.9a) [22].

This converter also has a similar downside to the boost converter. The buck converter can not emulate a smaller impedance than the load impedance, and therefore, it can not reach values near the open circuit voltage of the PV module [22] [23].

Buck-Boost converters are step-up and step-down DC-DC converters that can operate in both modes. This makes them more versatile than the previous two topologies, but also more complex and less efficient [22]. This converter uses an inductor to store energy when the transistor is in the ON state and the diode is reverse-biased. When the transistor is in the OFF state, the inductor releases the stored energy to the output through the diode, increasing or decreasing the output voltage (Figure 2.9c) [20].
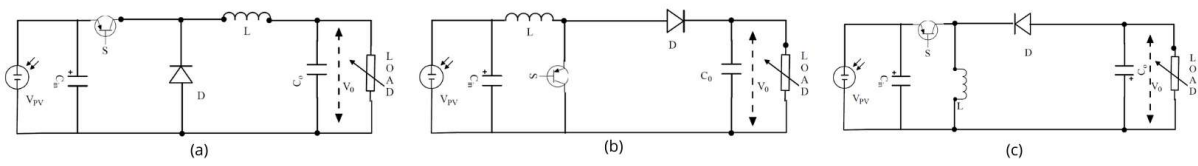

Figure 2.9: Buck (a), Boost (b) and Buck-Boost (c) DC-DC converters.

The conventional buck-boost converter produces an output voltage inverted with respect to the input which creates challenges on sensor measurements, driving circuit and isolation, consequently, it is unsuitable for the battery charging system [21].

An enhanced variant of the buck-boost converter is the CUK converter, illustrated in Figure 2.10a. The main characteristic of the CUK converter is that the currents through inductors L_1 and L_2 are equal, allowing the use of a common magnetic core, which helps reduce current ripple. However, a major drawback of this topology is that the entire load current must pass through the coupling capacitor C. In addition, the converter produces an inverted output voltage [21].

The issue of output voltage polarity inversion can be addressed by using a single-ended primary inductor converter (SEPIC), as shown in Figure 2.10b. This makes the SEPIC converter suitable for battery charging applications. Nevertheless, its main drawbacks are the high output current and voltage ripple which increases losses and electromagnetic interference (EMI) [24]. These limitations are mitigated by the ZETA converter, shown in Figure 2.10c, which provides improved output current characteristics while maintaining the same output voltage polarity as the SEPIC converter [13] [21].
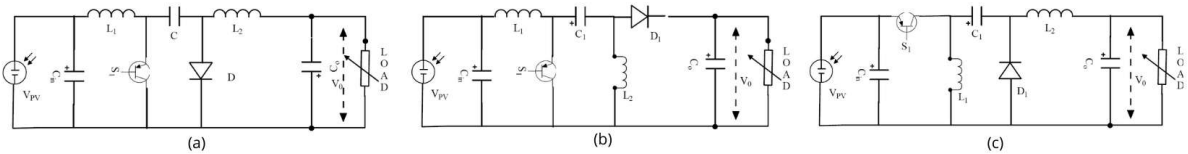

Figure 2.10: CUK (a), SEPIC (b) and ZETA (c) DC-DC converters.

2.4.3 Comparison between Non-isolated DC-DC converters

All the non-isolated DC-DC topologies explained before have their own advantages and disadvantages. The choice of the topology will depend on the specific application, the desired performance, and the available resources. To help with this choice, Table 2.3 shows a comparison between the most relevant characteristics of each topology [24]. The most significant advantages of each topology are highlighted.

Table 2.3: Comparison of non-isolated DC-DC topologies (good and important characteristics are highlighted).

Topology	Boost	Buck	Buck-Boost	ZETA	CUK	SEPIC
Electrical performance						
Efficiency	High	High	High	Medium/High	Medium	Medium
EMI	Low	Low	High	Medium	Medium	Medium
Input current ripple	Low	High	High	Low	Very low	Medium
Output current ripple	High	Low	High	Very low	Low	Medium
Output voltage ripple	Medium	Low	Medium	Low	Medium	High
Structural characteristics						
Circuit complexity	Low	Low	Low	Medium	Medium	Medium
Size	Low	Low	Low	Medium	Medium	Medium
Storage elements	1 L	1 L	1 L	2 L, 1 C	2 L, 1 C	2 L, 1 C
Switch stress	No	Yes	No	Yes	Yes	Yes
Functional aspects						
Type	Step-Up	Step-Down	Step-Down/Up	Step-Down/Up	Step-Down/Up	Step-Down/Up
Versatility	Low	Low	Medium	High	Medium	High
Inverted output	No	No	Yes	No	Yes	No
Reliability	High	High	High	Medium	Medium	Medium
Economic						
Cost	Low	Low	Low	Medium	Medium	Medium

For MPPT controllers, the choice is mainly governed by the possibility of operating at the MPP which is connected with the converter type, efficiency, cost (related to the number of storage elements), output voltage ripple.

The buck converter can be excluded from this comparison since in this project the solar panel voltage is lower than the battery voltage, therefore, a step-down converter is not suitable. However, when choosing between the boost and the step-up/down converters, there is a trade-off. The boost converter is simpler, cheaper and more efficient. On the other hand the step-down/up converters are more versatile since they can operate in a wide range of input voltages, which is interesting since the size of the solar panels and battery voltage can change.

Considering versatility as a key requirement, the Zeta converter emerges as the most efficient, non-inverted output option. Additionally, its low output voltage ripple makes it particularly well-suited for battery charging applications. Therefore, if versatility is prioritized, the ZETA converter would be the preferred choice among the step-up/down topologies. Also, the buck-boost converter is another alternative that provides versatility, but it has an inverted output voltage that will be a challenge for the sensors and driving circuits. On the other hand, if efficiency were prioritized, the boost converter would be the most suitable topology.

2.5 Battery charging techniques

As the demand for electronic devices and E-vehicles increases, the need for efficient, compact, and lightweight batteries has emerged. Among many existing technologies, lithium-ion batteries have one of the best energy-to-weight/volume ratios and, at this moment, it is the technology used in TSB batteries. But, like every other battery technology, they need to be charged properly to ensure their safety and longevity [25].

To charge these batteries properly, the MPPT algorithm can operate alone if an additional converter is used in series. But in most of MPPT chargers, the MPPT and the battery charging unit are integrated in the same converter. This way, the MPPT algorithm can adjust the operating point of the solar panel to extract the maximum power while the battery charging technique ensures that the battery is charged properly. A proper combination of both algorithms/techniques is essential to ensure both maximum energy extraction and battery safety.

There are several techniques to charge lithium-ion batteries, the most relevant for this use case being the constant current-constant voltage (CC-CV) method [26]. Also, it is widely used in commercial chargers due to its simplicity and effectiveness [27]. This method consists of two main phases (Figure 2.11). In the first phase, the battery is charged with a constant current until it reaches a predefined voltage limit (usually 4.2 V per cell). In the second phase, the voltage is held constant at this limit while the current gradually decreases as the battery approaches full charge. Once the current drops below a certain threshold, the charging process is terminated to prevent overcharging [27].

When employing the CC-CV charging technique with a MPPT controller, the initial Constant Current (CC) phase is regulated by the MPPT algorithm, which extracts the maximum available power from the solar panel limited by the maximum charging current. Once the Constant Voltage (CV) phase is reached, the MPPT function is disabled, and the power converter increases the solar panel voltage to progressively reduce the charging current while keeping the output voltage constant.
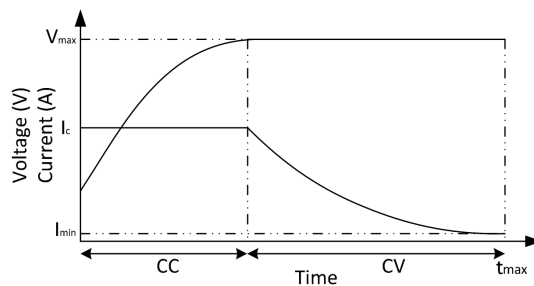

Figure 2.11: Charging profile of CC/CV [25].

More advanced high-performance battery charging techniques have been proposed in literature to reduce charging time without increasing the charging current, thereby preserving battery lifetime. However, these techniques generally introduce higher switching losses and increased system complexity. In the present application, the current generated by the photovoltaic panels is less than half of the maximum allowable battery charging current, consequently, the charging current is inherently limited by the solar panels rather than by the charging strategy. Furthermore, battery lifetime is not a critical concern in this project, as the battery is expected to undergo a limited number of charge cycles, not exceeding 20 cycles per year.

Therefore, the CC-CV charging method is considered the most suitable technique for this project, owing to its simplicity, effectiveness, and widespread adoption in commercial battery chargers.

Other charging techniques fall outside the scope of this work, however, some methods are briefly discussed in the references provided [26] [25] [27].

2.6   Processing unit

Several types of processing units can be considered for this project, including Microcontroller Units (MCUs), Field Programmable Gate Arrays (FPGAs), and Application-Specific Integrated Circuits (ASICs).

ASICs are custom-designed integrated circuits optimized for specific applications, offering high efficiency and performance. However, they are typically expensive and time-consuming to design and manufacture. Although commercially available ASICs, commonly referred to as Integrated Circuits (ICs), mitigate these drawbacks, they are usually made for a specific application and therefore not suitable for the high performance and flexibility required in this project, as discussed in Section 2.7.1.

FPGAs are reconfigurable devices capable of implementing custom digital circuits through programmable logic blocks based on look-up tables (LUTs) and interconnections [28]. Their main advantage lies in their inherent parallel processing capability, which enables high-performance operation. Nevertheless, FPGAs generally present high costs, high design complexity, and volatile configuration memory, requiring reprogramming after power loss [29, 30].

In contrast, MCUs are widely adopted in embedded systems due to their low cost, ease of use, and versatility. They integrate processing, memory, and peripherals in a single non-volatile device, simplifying hardware design and development. Although their sequential execution limits parallel processing performance compared to FPGAs, modern MCUs provide sufficient computational capability for many control and signal-processing tasks [29].

Considering the emphasis on low cost, reduced development time, and implementation simplicity, a MCU is selected for this application. Furthermore, the performance of current MCUs is adequate to meet the requirements of the MPPT algorithm and the battery charging strategy.

A Microcontroller Unit (MCU) typically consists of three fundamental components: a central processing unit (CPU), memory, and peripheral modules. The CPU executes program instructions and performs arithmetic and logical operations. Memory is generally divided into non-volatile memory (Flash) for program storage and volatile memory (SRAM) for data and runtime variables. Peripheral modules provide interfaces to the external environment and may include analog-to-digital converters (ADCs), timers, pulse-width modulation (PWM) units, communication interfaces (such as UART, SPI, I^2C and CAN), and general-purpose input/output (GPIO) ports. The integration of these components enables standalone operation without the need for extensive external circuitry [31].

When selecting a MCU for a specific application, the first factor to consider is to use an 8, 16, or 32 bit MCU. For this application, a 16-bit MCU would probably be sufficient, however to ensure future-proof and compatibility with other TSB systems, the choice is for a 32-bit MCU. Besides, nowadays, 32-bit MCUs are considered the industry standard since most embedded system Research and Development (R&D) effort is focused on 32-bit cores, and thus both architectures can achieve similar power consumption [32]. There are two main architectures for 32-bit MCUs: AVR and ARM. Being ARM, the most widely used architecture in the industry and the most advanced, it was chosen for this project [29].

Other important characteristics like clock speed, PWM resolution, communication protocols, memory capacity, power consumption, and cost, are not yet well-defined. The choice of MCU will be revisited in future stages of the project.

However, the STM32 family of MCU was already selected as it is the standard MCU used in TSB project and widely used in the industry. The STM32 family offers a wide range of solutions with different characteristics, making it suitable for various applications, including this project.

2.7 Commercial Options

To assess the feasibility of adopting a Off the shelf (OTS) solution, this section reviews existing commercial options for solar battery charging with MPPT capability. Both specialized ICs and complete commercial MPPT chargers are considered, and their electrical, functional, and economic characteristics are evaluated against the requirements of this project. The objective is to identify whether a commercially available solution can satisfy the constraints of the application or, alternatively, to justify the need for a custom-designed converter and control system.

2.7.1 Specialized ICs

Several commercially available Integrated Circuit (IC) are specifically designed for solar battery charging and MPPT applications. These devices are relevant to this project since, if suitable, they could significantly reduce design complexity by integrating functions such as DC-DC conversion, protection

mechanisms, and MPPT algorithm.

Table 2.4 summarizes four commonly used commercial ICs. Characteristics marked in red indicate incompatibilities with the project requirements, leading to the exclusion of the corresponding devices.

The BQ24650RVAT is a Stand-Alone Synchronous Buck Battery Charge Controller which implements a high-efficiency battery charger while also providing safety features. By adding a MCU to run a MPPT algorithm and current and voltage sensors, this IC can track the MPP of a solar panel, making it appropriate for applications with 12/24 V batteries and high-power panels, such as electric vehicles. However, it does not support the required 48 V battery voltage and is therefore unsuitable for this work.

The MAX20801TPBA+ and SPV1040TTR target low-power IoT applications with small batteries and solar panels. Both devices are unable to meet the 48 V output requirement, and their limited publicly available information on tracking speed further restricts performance evaluation.

The LT8491IUKJ#PBF offers a wide input and output voltage range, buck-boost operation, high efficiency, communication capabilities, and CC-CV charging. Despite these advantages, its reported MPPT tracking speed of up to 2 s is insufficient for the dynamic conditions of this application. Additionally, its I^2C interface would require an additional microcontroller to provide CAN communication, increasing system cost.

Table 2.4: Comparison of commercial specialized ICs (unsuitable characteristics are highlighted).

Model	BQ24650RVAT	MAX20801TPBA+	SPV1040TTR	LT8491IUKJ#PBF
Electrical specifications				
Input voltage	5 to 28 V	1.5 to 18 V	0.3 to 5.5 V	6 to 80 V
Output voltage	12 to 24 V	12.4 V	-0.3 to 5.5 V	1.3 to 80 V
Max output current	Externally limited	12 A	1.8 A	10 A
Switching frequency	600 kHz	Unknown	100 kHz	100 to 400 kHz
Electrical efficiency	95%	99.1% (max)	80 to 95%	95 to 99%
MPPT and control				
Algorithm	User input	Unknown	Unknown	P&O
Tracking accuracy	User dependent	99.9% (max)	Unknown	Unknown
Tracking speed	User dependent	Unknown	Unknown	1 to 2 s
Functional aspects				
Topology	Synchronous Buck	Synchronous Buck	Synchronous Boost	Buck-Boost
Communication	No	No	No	I^2C
Configurability	No	No	No	Yes
Charge profile	CC-CV	Unknown	Unknown	CC-CV
Extra hardware needed				
Transistors	Yes	No	No	Yes
Sensors	Yes	No	No	No
Storage elements	Yes	Yes	Yes	Yes
Economic				
Price	5.25 €	4.50 €	3.02 €	15-20 €

2.7.2 Commercial MPPT chargers

Several commercial MPPT chargers are available that can address the problem under analysis without requiring additional hardware. However, each solution presents limitations when evaluated against the project requirements. Table 2.5 summarizes selected commercial MPPT chargers, with red-marked

characteristics indicating incompatibilities.

The GVB-8-Li-CV(50.4) is a high-performance and fast MPPT charger, particularly suited for dynamic environments such as marine applications. It has been successfully used by TSB in previous projects, demonstrating high efficiency and reliability. Nevertheless, its lack of configurability, fixed output voltage, and high cost restrict its suitability for this application. Despite these drawbacks, it serves as a valuable reference design.

The Smart Solar MPPT 100/20, developed by Victron Energy, offers high efficiency, fast tracking, and integrated communication interfaces. However, it uses a buck topology that requires higher input voltages, making it incompatible with the small and distributed solar panel arrays used in the TSB application.

Other commercial solutions, such as the Rover Lite and MS4840N, provide acceptable performance but rely on communication protocols that are not compatible with the project requirements and offer limited technical documentation.

The Reboost V0.2.1 is an open source MPPT charger originally developed for automotive applications. While it provides flexibility and near adequate specifications, its reliance on expensive and discontinued components, along with the use of a boost topology, limits scalability and adaptability to potential future battery voltage changes.

Overall, none of the evaluated commercial MPPT chargers fully satisfy the technical, economic, and configurability requirements of this project, motivating the development of a custom solution.

Table 2.5: Comparison of commercial MPPT controllers (unsuitable characteristics are highlighted).

Model	GVB-8-Li-CV (50.4V)	Smart Solar MPPT 100/20	Reboost V0.2.1	Rover Lite	MS4840N
General information					
Brand	Gensun	Victron Energy	TPEE	Renogy	BougeRV
Type	Boost	Buck	Synchronous Boost	Boost	Boost
Control and communication					
Communication	No	VE.can and Bluetooth	Yes	Bluetooth and RS485	Bluetooth
Configurable	No	Yes	Yes	Yes	Yes
GUI	No	Yes	Yes	Yes	Yes
MPPT and charging					
Prog. battery voltage	No	Yes	Yes	non-lithium batteries	Yes
Tracking speed	15 Hz / 66.6(6) ms	Fast (unknown)	Programmable	Unknown	Unknown
Tracking efficiency	99%+ typical	Unknown	Programmable	99%	Unknown
Electrical efficiency	96-99% typical	98% peak	Unknown	97%	Unknown
Charger profile	CC-CV	Unknown	Programmable	Unknown	CC-CV
Hardware implementation					
MCU	ATtiny461A-U	Unknown	STM32G474	Unknown	Unknown
MCU Details	8-bit, RISC, 64 MHz	–	32-bit, Arm, 170 MHz	–	–
Transistor	FZT951	Unknown	GS61008T	Unknown	Unknown
Transistor type	PNP BJT	Unknown	GaN FETs	Unknown	Unknown
Economic					
Price	240 €	100-200 €	Components: 250-280 € PCB: 20-100 € Total: 270-380 €	300-350 €	120-160 €

3

Proposed Solution

This chapter presents the proposed solution developed to meet the technical, functional, and economic requirements identified in the previous chapters. It introduces the overall system architecture, detailing the interaction between the photovoltaic source, power conversion stage, control unit, and communication infrastructure. Additionally, the design methodology adopted for converter selection, control strategy, simulation, and experimental validation is described, providing a structured approach to the development and assessment of the proposed Maximum Power Point Tracker (MPPT) charger.

3.1 System architecture

The boat solar system is mainly composed of a battery, solar panels, and several MPPTs. Additionally, the Battery Management System (BMS) and sensors are used to maintain safety, Figure 3.1.
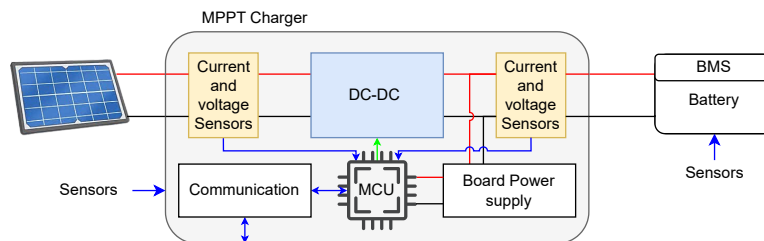

Figure 3.1: MPPT charger architecture.

This project aims to build an MPPT charger for São Guabriel 01 (SG01), which is one of the vessels built by Técnico Solar Boat (TSB), but TSB is continuously developing new boats with different batteries and different configurations of solar panels. With that in mind, the final solution needs to be versatile in terms of battery voltage and maximum ratings, which will provide savings over the years.

In terms of batteries, 3 different voltages were used in the past: 14.4 V, 21.6 V, and 50.4 V (nominal voltage). As for solar panels, the biggest solar panel array that TSB have ever built had 56 solar cells in series, which in total give a 40.94 V in open circuit and 6.382 A in short circuit (with Maxeon Gen 5 solar cells from SunPower). This will be considered as the limit size of the solar panel, and some margin will be added.

As for the MPPT charger, it is composed of a power supply cable to ensure steady DC voltage output

in the whole range of input voltages, a DC-DC converter alongside with a MCU which runs the MPPT algorithm to control the DC-DC converter taking into account the input measures of voltage and current, Figure 3.1.

The proposed system will use a step-down/up DC-DC converter to ensure output and input voltage flexibility, more specifically, a ZETA converter. As for the MPPT algorithm, a P&O will be initially used to simplify the work and further improved to a IncCond, however, the prototype needs to support other algorithms for further improvements. Thinking on the LUT algorithm, the proposed solution will be able to read both temperature and solar irradiance.

The communication with the system will be made by CAN communication with 1 Mbit/s of bus speed to connect every PCB to the same bus. CAN is the standard communication protocol used by TSB, however, when communicating with sensors there is more freedom and every other protocol can be used. The prototype will send messages to CAN bus with the data measured (voltage, current, temperature and irradiance) as well as calculated data such as power and electrical efficiency. Also, some additional information can be sent, such as status (error codes, charging, not charging, etc.) or warnings about solar panels health.

Within the CAN bus architecture, the BMS is also connected. The BMS is the main safety system of the battery. It measures input and output currents, cells temperatures, and voltages and decides if the battery is safe to use or not. Therefore, the final product does not need to provide these features. However, battery safety remains a priority and will be addressed in the proposed solution through protection mechanisms against overcurrent, overvoltage, and reverse polarity. Additionally, a CC-CV charging mode will be employed to ensure the safe charging of lithium-ion batteries.

3.1.1 Requirements summary

Considering all user requirements and adding some margin, the summary of the requirements is:

- Work with a wide range of battery voltage: from 14.4 V to 50.4 V;

- Input maximum rating: 300 W and 50 V;

- Input target: 105,12 W with 35 cells in series;

- Electrical efficiency: at least 85%;

- Fast tracking speed: less than 200 ms;

- High track accuracy: more than 95%;

- CAN communication: 1 Mbit/s and send status, power produced, current, voltage, efficiency and temperature;

- Load limits: overcurrent and overvoltage;

- Charging technique: CC-CV;

- Circuit protection: overcurrent, overvoltage, overtemperature, reverse polarity, ESD, etc.;

- MPPT algorithm: support different algorithms;

- Cost less than 150 € per unit.

To successfully complete this project, all the above requirements must be achieved in the final prototype.

3.2 Methodology

3.2.1 Simulations and Design

To satisfy the system requirements while maintaining operational flexibility, a step-up/down DC-DC converter topology is selected. This configuration enables operation under both low input and high output, or high input and low output voltage conditions. Furthermore, even when the solar panel and battery voltages are similar, this converter topology allows operation at the MPP, ensuring efficient energy harvesting.

Following the selection of the DC-DC converter topology, analytical design calculations and simulations will be carried out using MATLAB/Simulink to evaluate performance and optimize efficiency under varying operating conditions. This test should study the efficiency and voltage and current ripples from both input and output.

With respect to the MPPT algorithm, the prototype will be designed to support multiple MPPT algorithms to allow future extensibility and comparative evaluation. In addition to conventional methods, a hybrid algorithm previously proposed by António Neves in his master's thesis will be investigated. This algorithm combines a LUT with the P&O method using voltage and current measurements. In this work, the algorithm will be extended to include additional parameters, such as temperature and irradiance, to improve tracking accuracy and dynamic response.

All selected MPPT algorithms will be implemented and initially validated through simulations in MATLAB/Simulink before firmware implementation [5] [17]. The performance of each algorithm will be evaluated based on tracking speed and accuracy, which can be visualized by changing the environmental conditions in simulation and analyzing the power output [5] [14].

Also, research about how to implement low-power consumption voltage and current sensors will be conducted to find a cheap and accurate solution. A few solutions can be simulated in LTspice for precise tuning.

Finally, before testing the circuit in a prototype board or designing the PCB in Altium designer to later be manufactured, the MCU, sensors and additional hardware will be chosen according to the

22

specifications.

3.2.2 Experimental results and validation

Firstly, the correct functioning of the DC-DC converter and its efficiency will be tested with a resistive load and a power supply. By changing the input voltage and load resistance, several operating points can be tested, and the efficiency can be calculated by measuring input and output voltage and current.

At this stage, the current and voltage sensors will also be calibrated and tested to ensure accurate measurements.

As for the rest of the circuit, a laboratory control environment needs to be built with a closed box, and a light emitter device (for example a LED light). Inside this box the irradiance emitted by external sources, like lamps or the sun, will be reduced. The light emitter device should achieve irradiance close to the Standard Testing Conditions (STC), which is 1000 w/m^2.

The same can be achieved with the temperature using a simple heater and thermostat to maintain the system at a constant temperature or at STC conditions, which is 25 ℃.

This setup provides constant irradiance and temperature but can also provide variations to the environment variables, by changing the irradiance of LEDs with PWM or changing the reference signal of the thermostat. By applying abrupt variations (steps), to one of the variables, the controller speed and accuracy will be analyzed. To eliminate setup errors, an irradiance sensor and a temperature sensor should be installed inside the box for more accurate analysis of the results.

Finally, after laboratory validation of the prototype, real world testing will be conducted. The system will be connected to a photovoltaic panel and a battery and evaluated under varying environmental conditions. These tests aim to validate the laboratory results and to assess the overall performance of the proposed system under practical operating conditions. Then the robustness of the system can be tested by charging and discharging the battery several times, exposing the system to different temperatures and irradiance levels over a long period of time.

After all tests, the prototype will be installed in SG01 alongside with the previous used MPPT controllers to compare the performance in real world conditions.

4 Preliminary Work

In order to get familiar with the tools needed for the development of the project, some basic tests were conducted. In this section, a brief introduction to simulation tools and Hardware tests are presented.

4.1 Simulations

MATLAB/Simulink is widely used for simulating the behavior of MPPT chargers. It enables PV panel modeling by defining environmental conditions such as temperature and irradiance, as well as electrical parameters including open-circuit voltage, short-circuit current, and temperature coefficients. Using the Simscape Electrical library, the DC-DC converter and battery can also be modeled, allowing the simulation to closely approximate the behavior of the real system.

Despite this, simulations rely on simplifying assumptions, which may lead to discrepancies between simulated and real-world performance. Therefore, simulation results must be carefully analyzed and validated using experimental hardware.

Figure 4.1 shows the MATLAB/Simulink model implemented with a boost converter and the P&O algorithm. This model was developed primarily to familiarize, with the simulation environment and identify modeling challenges, and its structure to further refinement.

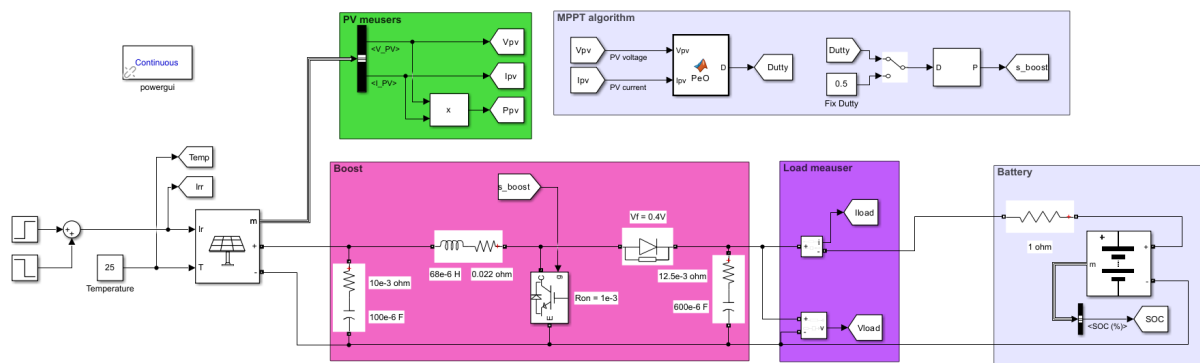**Figure 4.1:** Matlab/Simulink system model with Boost Converter and P&O algorithm.

The objective was successfully accomplished, with good results. Figure 4.2,4.3 and 4.4 show the results of the presented model with a solar irradiance step from 0 $\mathrm{w/m}^2$ to 1000 $\mathrm{w/m}^2$ at 0 seconds and from 1000 $\mathrm{w/m}^2$ to 500 $\mathrm{w/m}^2$ at 0.30 seconds. The temperature was kept constant at 25 ºC.
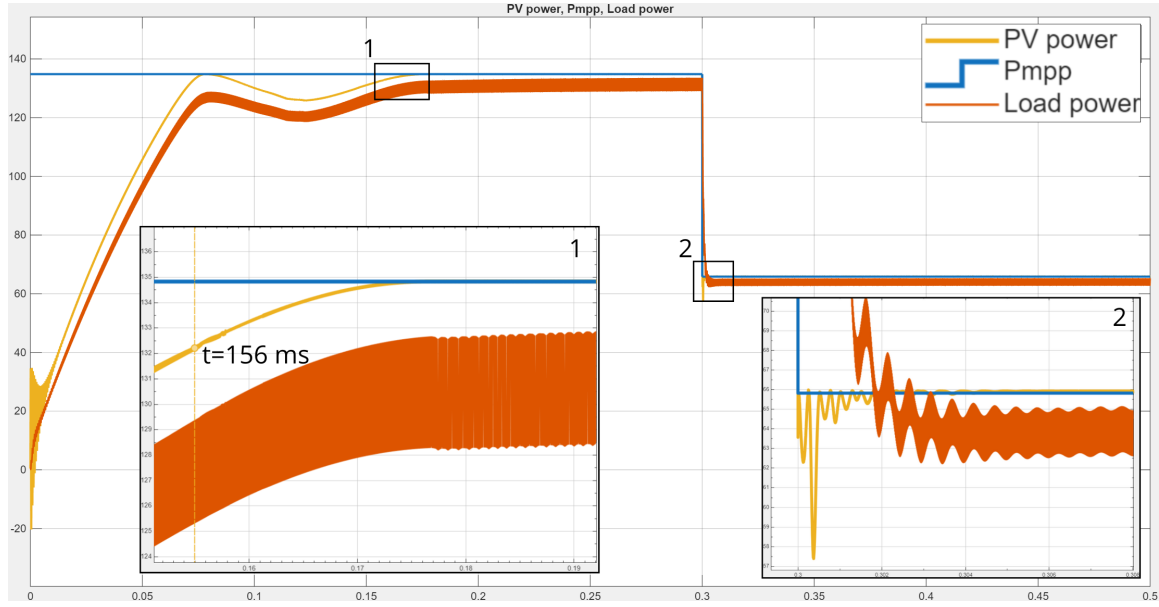
Figure 4.2: Matlab/Simulink results.
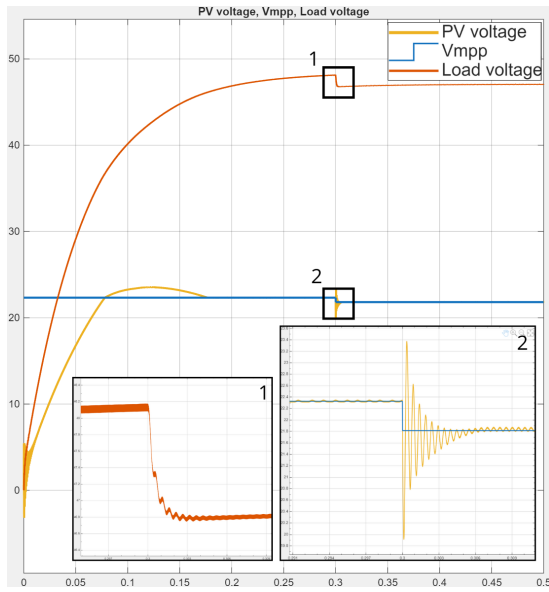
Figure 4.3
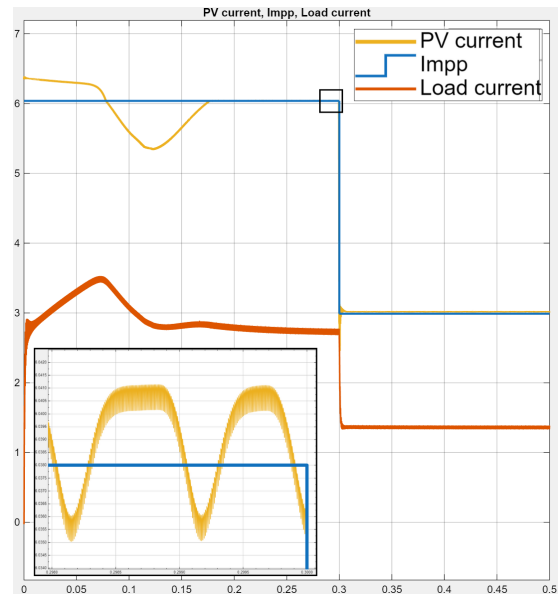
Figure 4.4

The Maximum Power Point (MPP) of the given solar panel ($V_{mpp} = 22.33$ V, $I_{mpp} = 6.038$ A and $P_{mpp} = 134.829$ W) was successfully tracked with a simple algorithm. The maximum tracking speed achieved was 156ms with the output capacitor unloaded at the first step, however a speed of 1ms was achieved in the second step. These results are acceptable for this initial stage, but will be studied further in future work. Also, the MPPT algorithm was able to achieve a high accuracy, close to 100%, Figure 4.2 however, the algorithm oscillates around the MPP due to the P&O method characteristics. This behavior

was particularly evident during the second operating step, where a voltage oscillation of 15.6% around the MPP was measured (Figure 4.3).

As for the efficiency of the boost converter, it achieved a maximum of 97.34% at full load, which is a high value for this kind of converter, but it is just a simulation, and real values will be lower.

4.2   Hardware tests

Since the use of an STM32 is one of the requirements of TSB to comply with their standards, some research and tests were also performed to get familiar with the software tools and the requirements of the MCU.

The tests were carried out with a cheap development board called Blue Pill, which accommodates a STM32F103C8T6 (Figure 4.5). As this is one of the cheapest boards on the market, the specifications are not high-end. However, it was suitable for the aim of these tests.

The STM32F103C8T6 has an ARM Cortex-M3 32-bit core running at up to 72 MHz, providing sufficient processing performance for real-time control and signal-processing tasks. It integrates two 12-bit ADCs with a maximum sampling rate of approximately 1 million samples per second and up to 16 multiplexed analog input channels, while no internal DAC is available. The device includes several general-purpose and advanced timers capable of generating PWM signals, with maximum PWM frequencies limited by the 72 MHz timer clock and the selected resolution. Housed in a 48-pin package, it offers up to around 37 configurable GPIO pins. In terms of communication interfaces, the MCU supports multiple USARTs, SPI and I^{2}C peripherals, as well as a Full-Speed USB 2.0 device interface, making it suitable for a wide range of embedded communication requirements.

The tests conducted were based on online examples, which allowed the evaluation of several functionalities of this MCU, including timers, interrupts, basic GPIO operations, PWM generation, ADC usage, and communication interfaces such as USB, CAN, serial, and I^{2}C.
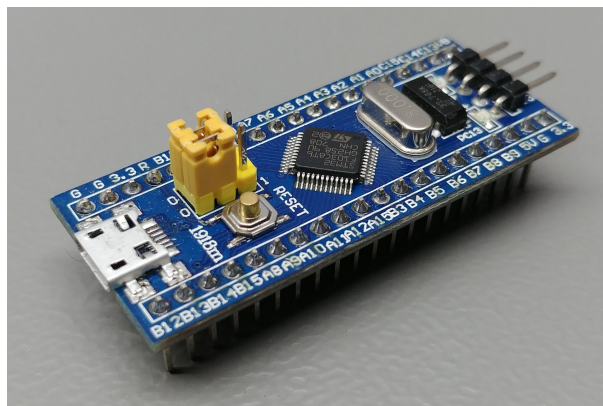

Figure 4.5: Blue Pill development board.

5

Planning and Scheduling

The establishment of deadlines and a structured work plan are essential for monitoring project progress and ensuring efficient task execution. To this end, a Gantt chart was developed and is presented in Fig. 5.1, in which the work is divided into tasks and stages distributed throughout the year.
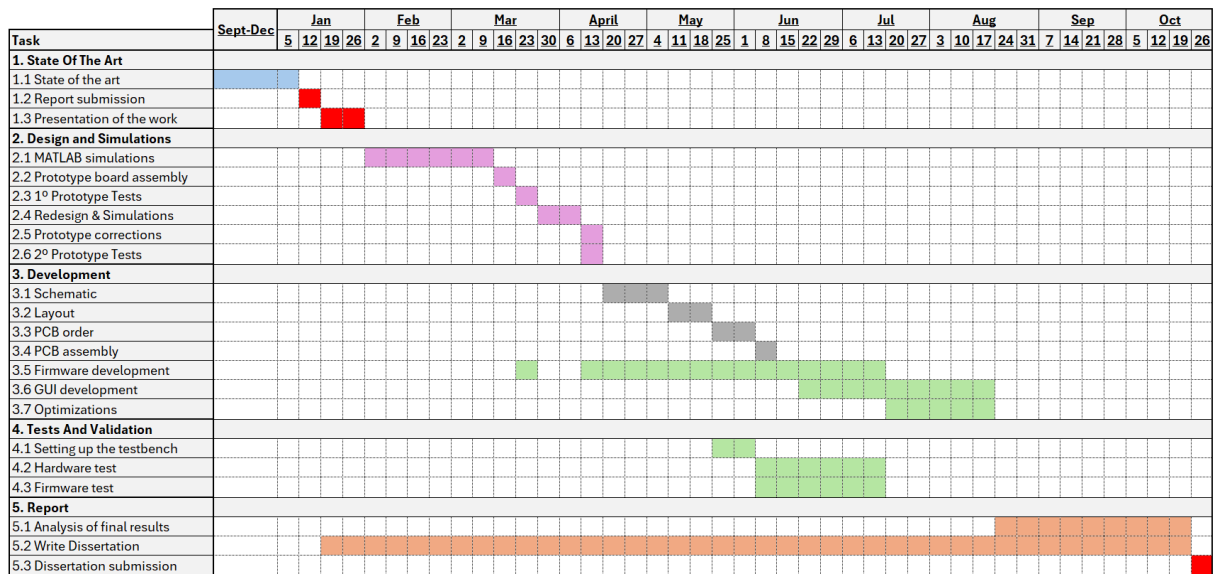
Task	Sept-Dec	Jan	Feb	Mar	April	May	Jun	Jul	Aug	Sep	Oct
		5 12 19 26	2 9 16 23	2 9 16 23 30	6 13 20 27	4 11 18 25	1 8 15 22 29	6 13 20 27	3 10 17 24 31	7 14 21 28	5 12 19 26
1. State Of The Art											
1.1 State of the art											
1.2 Report submission											
1.3 Presentation of the work											
2. Design and Simulations											
2.1 MATLAB simulations											
2.2 Prototype board assembly											
2.3 1º Prototype Tests											
2.4 Redesign & Simulations											
2.5 Prototype corrections											
2.6 2º Prototype Tests											
3. Development											
3.1 Schematic											
3.2 Layout											
3.3 PCB order											
3.4 PCB assembly											
3.5 Firmware development											
3.6 GUI development											
3.7 Optimizations											
4. Tests And Validation											
4.1 Setting up the testbench											
4.2 Hardware test											
4.3 Firmware test											
5. Report											
5.1 Analysis of final results											
5.2 Write Dissertation											
5.3 Dissertation submission											

Figure 5.1: Gantt Chart of the work to be performed.

The work started with the State-of-the-Art research presented in this document that will be further expanded in the dissertation work

Then, as described in previous sections, some simulations will be developed to evaluate the proposed solution. After a reliable and robust solution is achieved, a prototype will be built on a prototype board to validate the simulations without spending a lot of money and time.

When a successful prototype is achieved, the PCB will be designed, fabricated, assembled, and tested.

Finally, firmware specifically made for the Maximum Power Point Tracker (MPPT) charger will be made alongside with hardware test and Graphical User Interface (GUI) development.

After all hardware and software design, the board will be tested alongside with SG01 in real world conditions and the data will be analyzed, and documented in the dissertation document.

Bibliography

[1] Our World in Data, "Electricity mix," 2025, accessed: 2025-11-24. [Online]. Available: https://ourworldindata.org/electricity-mix

[2] U. Shahira, S. Z. Islam, R. b. Omar, M. L. Othman, S. Z. Said, and J. Uddin, "Electrical design of solar-powered recreational boat in malaysia," in *2022 IEEE International Conference on Power and Energy (PECon)*, 2022, pp. 138–143.

[3] International Council on Clean Transportation (ICCT), "Transport could burn up the eu's entire carbon budget," n.d., accessed: 2025-11-24. [Online]. Available: https://theicct.org/transport-could-burn-up-the-eus-entire-carbon-budget/

[4] D. Hohm and M. Ropp, "Comparative study of maximum power point tracking algorithms using an experimental, programmable, maximum power point tracking test bed," in *Conference Record of the Twenty-Eighth IEEE Photovoltaic Specialists Conference - 2000 (Cat. No.00CH37036)*, 2000, pp. 1699–1702.

[5] B. Bendib, H. Belmili, and F. Krim, "A survey of the most used mppt methods: Conventional and advanced algorithms applied for photovoltaic systems," *Renewable and Sustainable Energy Reviews*, vol. 45, pp. 637–648, 2015.

[6] M. Abdulazeez and I. Iskender, "Simulation and experimental study of shading effect on series and parallel connected photovoltaic pv modules," in *2011 7th International Conference on Electrical and Electronics Engineering (ELECO)*, 2011, pp. I–28–I–32.

[7] H. Häberlin, *Photovoltaics: system design and practice.* John Wiley & Sons, 2012.

[8] K. Karjust, J. Majak, and P. Tšukrejev, "Experimental evaluation and numerical modelling of the quality of photovoltaic modules," *Proceedings of the Estonian Academy of Sciences*, vol. 70, p. 477, 11 2021.

[9] T. Esram and P. L. Chapman, "Comparison of photovoltaic array maximum power point tracking techniques," *IEEE Transactions on Energy Conversion*, vol. 22, no. 2, pp. 439–449, 2007.

[10] B. Subudhi and R. Pradhan, "A comparative study on maximum power point tracking techniques for photovoltaic power systems," *IEEE Transactions on Sustainable Energy*, vol. 4, no. 1, pp. 89–98, 2013.

[11] K. Kobayashi, H. Matsuo, and Y. Sekine, "A novel optimum operating point tracker of the solar cell power supply system," in *2004 IEEE 35th Annual Power Electronics Specialists Conference (IEEE Cat. No.04CH37551)*, vol. 3, 2004, pp. 2147–2151 Vol.3.

[12] B. M. Ali Chermitti, Omar Boukli-hacene, "Improvement of the ìperturb and observeî mppt algorithm in a photovoltaic system under rapidly changing climatic conditions," *International Journal of Computer Applications*, vol. 56, no. 12, pp. 11–16, October 2012.

[13] F. Dwi Murdianto, A. Rofiq Nansur, and Y. Heriani, "Comparison of first order differential algorithm, perturb and observe (p&o) and newton raphson methods for pv application in dc microgrid isolated system," in *2018 International Seminar on Application for Technology of Information and Communication*, 2018, pp. 145–150.

[14] J. K. Udavalakshmi and M. S. Sheik, "Comparative study of perturb & observe and look-up table maximum power point tracking techniques using matlabisimulink," in *2018 International Conference on Current Trends towards Converging Technologies (ICCTCT)*, 2018, pp. 1–5.

[15] O. Wasynezuk, "Dynamic behavior of a class of photovoltaic power systems," *IEEE Transactions on Power Apparatus and Systems*, vol. PAS-102, no. 9, pp. 3031–3037, 1983.

[16] E. Roman, R. Alonso, P. Ibanez, S. Elorduizapatarietxe, and D. Goitia, "Intelligent pv module for grid-connected pv systems," *IEEE Transactions on Industrial Electronics*, vol. 53, no. 4, pp. 1066–1073, 2006.

[17] A. Safari and S. Mekhilef, "Simulation and hardware implementation of incremental conductance mppt with direct control method using cuk converter," *IEEE Transactions on Industrial Electronics*, vol. 58, no. 4, pp. 1154–1161, 2011.

[18] Flex Power Modules, "Isolated vs non-isolated power converters — an overview," Online, n.d., accessed: 2025-12-09. [Online]. Available: https://flexpowermodules.com/isolated-vs-non-isolated-power-converters-an-overview

[19] I. Alhurayyis, A. Elkhateb, and J. Morrow, "Isolated and nonisolated dc-to-dc converters for medium-voltage dc networks: A review," *IEEE Journal of Emerging and Selected Topics in Power Electronics*, vol. 9, no. 6, pp. 7486–7500, 2021.

[20] F. Mocci and M. Tosi, "Comparison of power converter technologies in photovoltaic applications," in *Proceedings. Electrotechnical Conference Integrating Research, Industry and Education in Energy and Communication Engineering'*, 1989, pp. 11–15.

[21] I. Yadav and S. K. Maurya, "The non-isolated dc to dc converters for mppt controller based on the load line analysis used for solar pv applications," in *2021 Emerging Trends in Industry 4.0 (ETI 4.0)*, 2021, pp. 1–5.

[22] M. A. Chewale, R. A.Wanjari, V. B.Savakhande, and P. R.Sonawane, "A review on isolated and non-isolated dc-dc converter for pv application," in *2018 International Conference on Control, Power, Communication and Computing Technologies (ICCPCCT)*, 2018, pp. 399–404.

[23] E. Duran, J. Galan, M. Sidrach-de Cardona, and J. Andujar, "A new application of the buck-boost-derived converters to obtain the i-v curve of photovoltaic modules," in *2007 IEEE Power Electronics Specialists Conference*, 2007, pp. 413–417.

[24] S. Yadav, S. Mishra, and Garima, "Comparative analysis of non-isolated dc-dc converters for solar-photovoltaic system," in *2021 8th International Conference on Signal Processing and Integrated Networks (SPIN)*, 2021, pp. 880–885.

[25] W. Shen, T. T. Vo, and A. Kapoor, "Charging algorithms of lithium-ion batteries: An overview," in *2012 7th IEEE Conference on Industrial Electronics and Applications (ICIEA)*, 2012, pp. 1567–1572.

[26] A. Al-Haj Hussein and I. Batarseh, "A review of charging algorithms for nickel and lithium battery chargers," *IEEE Transactions on Vehicular Technology*, vol. 60, no. 3, pp. 830–838, 2011.

[27] J. Fattal and P. B. Dib Nabil Karami, "Review on different charging techniques of a lithium polymer battery," in *2015 Third International Conference on Technological Advances in Electrical, Electronics and Computer Engineering (TAEECE)*, 2015, pp. 33–38.

[28] J. Rose, A. El Gamal, and A. Sangiovanni-Vincentelli, "Architecture of field-programmable gate arrays," *Proceedings of the IEEE*, vol. 81, no. 7, pp. 1013–1029, 1993.

[29] Ampheo, "Fpga vs microcontroller — which one is the best?" Online, n.d., accessed: 2025-12-27. [Online]. Available: https://www.ampheo.com/blog/fpga-vs-microcontroller-which-one-is-the-best?srsltid=AfmBOopUrXMH48pNvNOAu3BpPxHq9w6yi1EQKHTsduIsT0pLxEXMXtrh

[30] N. Khaehintung, T. Wiangtong, and P. Sirisuk, "Fpga implementation of mppt using variable step-size p&o algorithm for pv applications," 2006, pp. 212–215.

[31] IBM, "Microcontroller," Online, n.d., accessed: 2025-12-27. [Online]. Available: https://www.ibm.com/think/topics/microcontroller

[32] Embedded.com, "Upgrading 8- and 16-bit mcu designs 32-bit mcu architectures," Online, n.d., accessed: 2025-12-27. [Online]. Available: https://www.embedded.com/upgrading-8-and-16-bit-mcu-designs-32-bit-mcu-architectures/